Chemical Science

ROYAL SOCIETY OF CHEMISTRY

EDGE ARTICLE

View Article Online
View Journal | View Issue

Cite this: *Chem. Sci.*, 2022, **13**, 5938

All publication charges for this article have been paid for by the Royal Society of Chemistry

Received 22nd March 2022
Accepted 24th April 2022

DOI: 10.1039/d2sc01677j

rsc.li/chemical-science

Ligand-promoted palladium-catalyzed β-methylene C–H arylation of primary aldehydes†

Ke Yang,[a] Zhi Li,[a] Chong Liu,[b] Yunjian Li,[a] Qingyue Hu,[a] Mazen Elsaid,[b] Bijin Li,[b] Jayabrata Das,[d] Yanfeng Dang,*[c] Debabrata Maiti*[d] and Haibo Ge*[b]

The transient directing group (TDG) strategy allowed long awaited access to the direct β-C(sp^3)–H functionalization of unmasked aliphatic aldehydes *via* palladium catalysis. However, the current techniques are restricted to terminal methyl functionalization, limiting their structural scopes and applicability. Herein, we report the development of a direct Pd-catalyzed methylene β-C–H arylation of linear unmasked aldehydes by using 3-amino-3-methylbutanoic acid as a TDG and 2-pyridone as an external ligand. Density functional theory calculations provided insights into the reaction mechanism and shed light on the roles of the external and transient directing ligands in the catalytic transformation.

Simple aliphatic functional groups enrich the skeletal backbones of many natural products, pharmaceuticals, and other industrial materials, influencing the utility and applications of these substances and dictating their reactivity and synthetic modification pathways. Aliphatic aldehydes are some of the most ubiquitous structural units in organic materials.[1] Their relevance in nature and industry alike, combined with their reactivity and synthetic versatility, attracted much attention from the synthetic organic and medicinal chemistry communities over the years (Fig. 1).[2] Efficient means to the functionalization of these molecules have always been highly sought after.

Traditionally, scientists have utilized the high reactivity of the aldehyde moiety in derivatizing a variety of functional groups by the means of red-ox and nucleophilic addition reactions. The resourceful moiety was also notoriously used to install functional groups at the α-position *via* condensation and substitution pathways.[3] Although β-functionalization is just as robust, it has generally been more restrictive as it often requires the use of α,β-unsaturated aldehydes.[4,5] Hence, transition metal catalysis emerged as a powerful tool to access β-functionalization in saturated aldehydes.[6] Most original examples of metal-catalyzed β-C–H functionalization of aliphatic aldehydes required the masking of aldehydes into better metal coordinating units since free unmasked aldehydes could not form stable intermediates with metals like palladium on their own.[7] Although the masking of the aldehyde moiety into an oxime, for example, enabled the formation of stable 5-membered palladacycles, affording β-functionalized products, this system requires the installation of the directing group prior to the functionalization, as well as the subsequent unmasking upon the reaction completion, compromising the step economy and atom efficiency of the overall process.[8] Besides, some masking and unmasking protocols might not be compatible with select substrates, especially ones rich in functional groups. As a result, the development of a one-step direct approach to the β-C–H functionalization of free aliphatic aldehydes was a demanding target for synthetic chemists.

α-Amino acids have been demonstrated as effective transient directing groups (TDGs) in the remote functionalization of *o*-alkyl benzaldehydes and aliphatic ketones by the Yu group in 2016.[9] Shortly after, our group disclosed the first report on the direct β-C–H arylation of aliphatic aldehydes using 3-aminopropanoic acid or 3-amino-3-methylbutanoic acid as a TDG.[10]

[a]*Jiangsu Key Laboratory of Advanced Catalytic Materials & Technology, School of Petrochemical Engineering, Changzhou University, Jiangsu 213164, China*

[b]*Department of Chemistry and Biochemistry, Texas Tech University, Lubbock, TX 79409-1061. E-mail: Haibo.Ge@ttu.edu*

[c]*Tianjin Key Laboratory of Molecular Optoelectronic Sciences, Department of Chemistry, School of Science, Tianjin University, Tianjin 300072. E-mail: yanfeng.dang@tju.edu.cn*

[d]*Department of Chemistry and Interdisciplinary Program in Climate Studies, Indian Institute of Technology Bombay, Mumbai 400076. E-mail: dmaiti@iitb.ac.in*

† Electronic supplementary information (ESI) available. See https://doi.org/10.1039/d2sc01677j

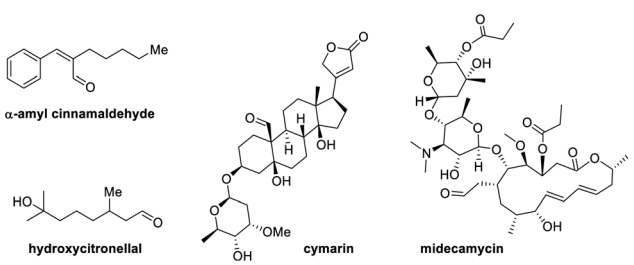

Fig. 1 Select aliphatic aldehyde-containing medicines and biologically active molecules.

The TDG was found to play a similar role to that of the oxime directing group by binding to the substrate *via* reversible imine formation, upon which, it assists in the assembly of a stable palladacycle, effectively functionalizing the β-position.[11] Since the binding of the TDG is reversible and temporary, it is automatically removed upon functionalization, yielding an efficient and step-economic transformation. This work was succeeded by many other reports that expanded the reaction and the TDG scopes.[12–14] However, this system suffers from a significant restriction that demanded resolution; only substitution of methyl C–H bonds of linear aldehydes was made possible *via* this approach (Scheme 1a–e). The steric limitations caused by incorporating additional groups at the β-carbon proved to compromise the formation of the palladacycle intermediate, rendering the subsequent functionalization a difficult task.[12]

Encouraged by the recent surge in use of 2-pyridone ligands to stabilize palladacycle intermediates,[15,16] we have successfully developed the first example of TDG-enabled Pd-catalyzed methylene β-C–H arylation in primary aldehydes *via* the assistance of 2-pyridones as external ligands (Scheme 1f). The incorporation of 2-pyridones proved to lower the activation energy of the C–H bond cleavage, promoting the formation of the intermediate palladacycles even in the presence of relatively bulky β-substituents.[17] This key advancement significantly broadens the structural scopes and applications of this process and promises future asymmetric possibilities, perhaps *via* the use of a chiral TDG or external ligand or both. Notably, a closely related work from Yu's group was published at almost the same time.[18]

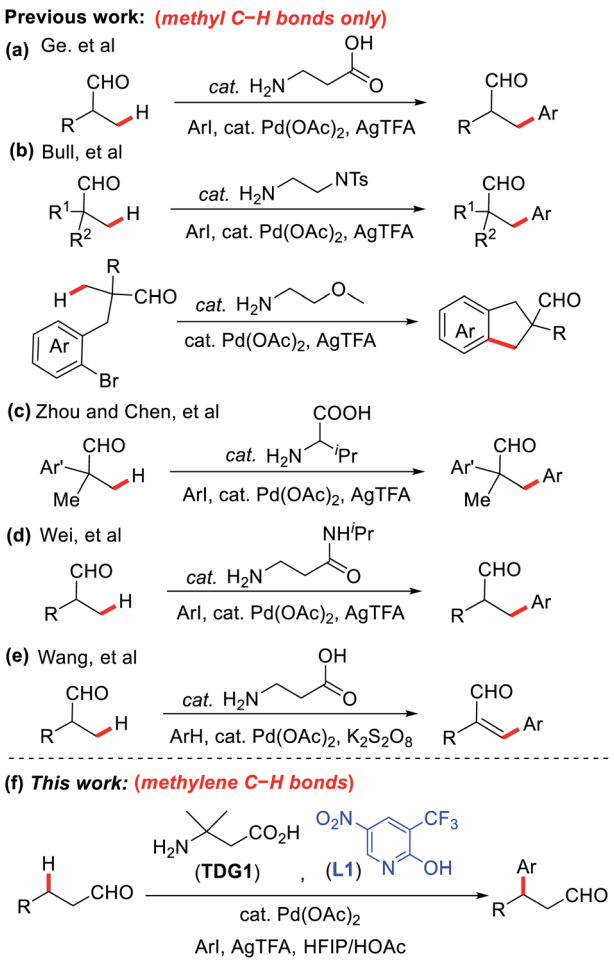

Scheme 1 Pd-catalyzed β-C–H bond functionalization of aliphatic aldehydes enabled by transient directing groups.

We commenced our investigation of the reaction parameters by employing *n*-pentanal (**1a**) as an unbiased linear aldehyde and 4-iodoanisole (**2a**) in the presence of catalytic $Pd(OAc)_2$ and stoichiometric AgTFA, alongside 3-amino-3-methylbutanoic acid (**TDG1**) and 3-(trifluoromethyl)-5-nitropyridin-2-ol (**L1**) at 100 °C (Table 1). Initial solvent screening results (entries 1–5) suggested that an optimal 9 : 1 volumetric ratio of HFIP to HOAc (2.0 mL total) afforded the desired product **3a** in 47% NMR yield. Further studies indicated that an increased loading of **L1** (from 30% to 60%) and **TDG1** (from 40% to 60%) improved the NMR yield of **3a** to 70% (entries 6–9). The subsequent screening of Pd(II) sources proved $Pd(OAc)_2$ to be the optimal catalyst, while $Pd(TFA)_2$, $PdCl_2$ and $PdBr_2$ provided only moderate yields (entries 10–12). Notably, a significantly lower yield was observed in the absence of the 2-pyridone ligand, and no desired product was isolated altogether in the absence of the TDG (entries 13 and 14). The incorporation of 15 mol% Pd catalyst was deemed necessary after only 55% yield of **3a** was obtained when 10 mol% loading of $Pd(OAc)_2$ was instead used (entry 15).

To advance our optimization of the reaction conditions, a variety of 2-pyridones and TDGs were tested (Scheme 2). Originally, pyridine-2(1*H*)-one (**L2**) was examined as the external ligand, but it only yielded the product (**3a**) in 7% NMR yield. Similarly, other mono- and di-substituted 2-pyridone ligands (**L3–L10**) also produced low yields, fixating **L1** as the optimal external ligand. Next, various α- and β-amino acids (**TDG1–10**) were evaluated, yet **TDG1** persisted as the optimal transient directing group. These amino acid screening results also suggest that a [5,6]-bicyclic palladium species is likely the key intermediate in this protocol since only β-amino acids were found to provide appreciable yields, whereas α-amino acids failed to yield more than trace amounts of the product. The supremacy of **TDG1** when compared to other β-amino acids is presumably due to the Thorpe–Ingold effect that perhaps helps facilitate the C–H bond cleavage and stabilize the [5,6]-bicyclic intermediate further.

With the optimized reaction conditions in hand, substrate scope study of primary aliphatic aldehydes was subsequently carried out (Scheme 3). A variety of linear primary aliphatic aldehydes bearing different chain lengths provided the corresponding products **3a–e** in good yields. Notably, relatively sterically hindered methylene C–H bonds were also functionalized effectively (**3f** and **3g**). Additionally, 4-phenylbutanal gave rise to the desired product **3h** in a highly site-selective manner, suggesting that functionalization of the methylene β-C–H bond is predominantly favored over the more labile benzylic C–H bond. It is noteworthy that the amide group was also well-tolerated and the desired product **3j** was isolated in 60% yield. As expected, with *n*-propanal as the substrate, β-mono-

Table 1 Optimization of reaction conditions[a]

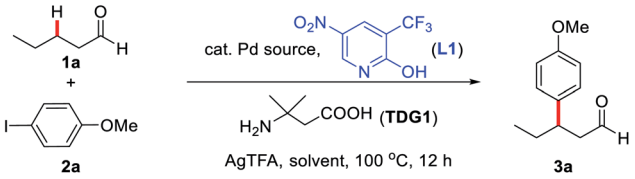

Entry	Pd source	L (mol%)	TDG1 (mol%)	Solvent (v/v, mL)	Yield (%)
1	$Pd(OAc)_2$	L1 (30)	TDG1 (40)	HFIP	30
2	$Pd(OAc)_2$	L1 (30)	TDG1 (40)	AcOH	<5
3	$Pd(OAc)_2$	L1 (30)	TDG1 (40)	HFIP/AcOH (1 : 1)	28
4	$Pd(OAc)_2$	L1 (30)	TDG1 (40)	HFIP/AcOH (9 : 1)	47
5	$Pd(OAc)_2$	L1 (30)	TDG1 (40)	HFIP/AcOH (1 : 9)	<5
6	$Pd(OAc)_2$	L1 (30)	TDG1 (60)	HFIP/AcOH (9 : 1)	50
7	$Pd(OAc)_2$	L1 (30)	TDG1 (80)	HFIP/AcOH (9 : 1)	25
8	$Pd(OAc)_2$	L1 (60)	TDG1 (60)	HFIP/AcOH (9 : 1)	70(68)[b]
9	$Pd(OAc)_2$	L1 (75)	TDG1 (60)	HFIP/AcOH (9 : 1)	51
10	$Pd(TFA)_2$	L1 (60)	TDG1 (60)	HFIP/AcOH (9 : 1)	60
11	$PdCl_2$	L1 (60)	TDG1 (60)	HFIP/AcOH (9 : 1)	52
12	$PdBr_2$	L1 (60)	TDG1 (60)	HFIP/AcOH (9 : 1)	54
13	$Pd(OAc)_2$	—	TDG1 (60)	HFIP/AcOH (9 : 1)	9
14	$Pd(OAc)_2$	L1 (60)	—	HFIP/AcOH (9 : 1)	0
15[c]	$Pd(OAc)_2$	L1 (60)	TDG1 (60)	HFIP/AcOH (9 : 1)	55

[a] Reaction conditions: **1a** (0.2 mmol), **2a** (0.4 mmol), Pd source (15 mol%), AgTFA (0.3 mmol), **L1**, **TDG1**, solvent (2.0 mL), 100 °C, 12 h. Yields are based on **1a**, determined by ^{1}H-NMR using dibromomethane as an internal standard. [b] Isolated yield. [c] $Pd(OAc)_2$ (10 mol%).

(**3k1**) and β,β-disubstituted products (**3k2**) were isolated in 22% and 21% yields respectively. However, in the absence of the key external 2-pyridone ligand, β-monosubstituted product (**3k1**) was obtained exclusively, albeit with a low yield, indicating preference for functionalizing the β-C(sp^3)–H bond of the methyl group over the benzylic methylene group.

Next, substrate scope study on aryl iodides was surveyed (Scheme 4). Iodobenzenes bearing either an electron-donating or electron-withdrawing group at the *para*-, *meta*-, or *ortho*-position were all found compatible with our catalytic system (**3l–3ah**). Surprisingly, *ortho*-methyl- and fluoro-substituted aryl iodides afforded the products in only trace amounts. However, aryl iodide with *ortho*-methoxy group provided the desired product **3ac** in a moderate yield. Notably, a distinctive electronic effect pattern was not observed in the process. It should be mentioned that arylated products bearing halogen, ester, and cyano groups could be readily converted to other molecules, which significantly improves the synthetic applicability of the process. Delightfully, aryl iodide-containing natural products like ketoprofen, fenchol and menthol were proven compatible, supplying the corresponding products in moderate yields. Unfortunately, (hetero)aryl iodides including 2-iodopyridine, 3-iodopyridine, 4-iodopyridine and 4-iodo-2-chloropyridine failed to produce the corresponding products. Although our protocol provides a novel and direct pathway to construct β-arylated primary aliphatic aldehydes, the yields of most examples are modest. The leading reasons for this compromise are the following: (1) aliphatic aldehydes are easily decomposed or oxidized to acids; (2) some of the prepared β-arylated aldehyde products may be further transformed into the corresponding α,β-unsaturated aldehydes.

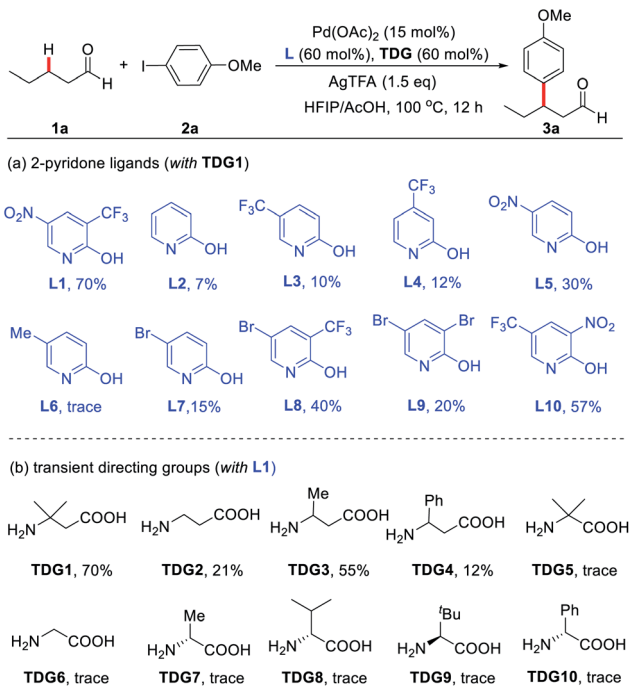

Scheme 2 Optimization of 2-pyridone ligands and transient directing groups.

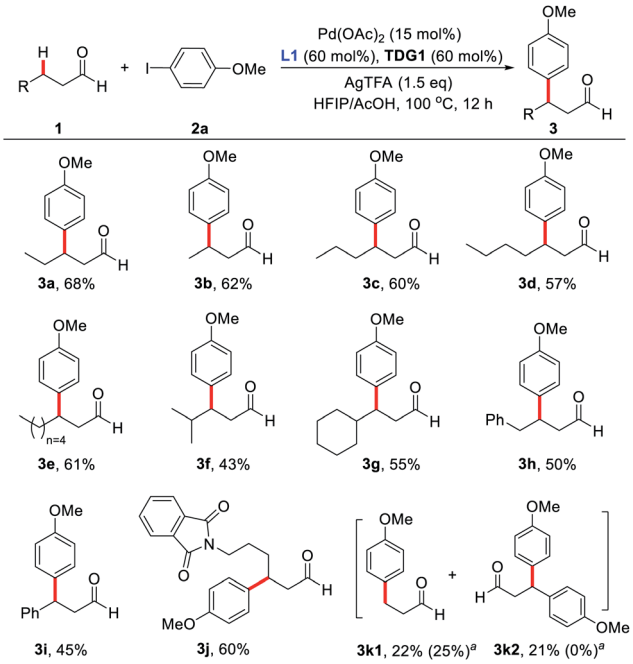

Scheme 3 Scope of primary aliphatic aldehydes. Reaction conditions: **1** (0.2 mmol), **2a** (0.4 mmol), $Pd(OAc)_2$ (15 mol%), AgTFA (0.3 mmol), **L1** (60 mol%), **TDG1** (60 mol%), HFIP (1.8 mL), HOAc (0.2 mL), 100 °C, 12 h. Isolated yields. [a]**L1** (60 mol%) was absent and yields are given in parentheses.

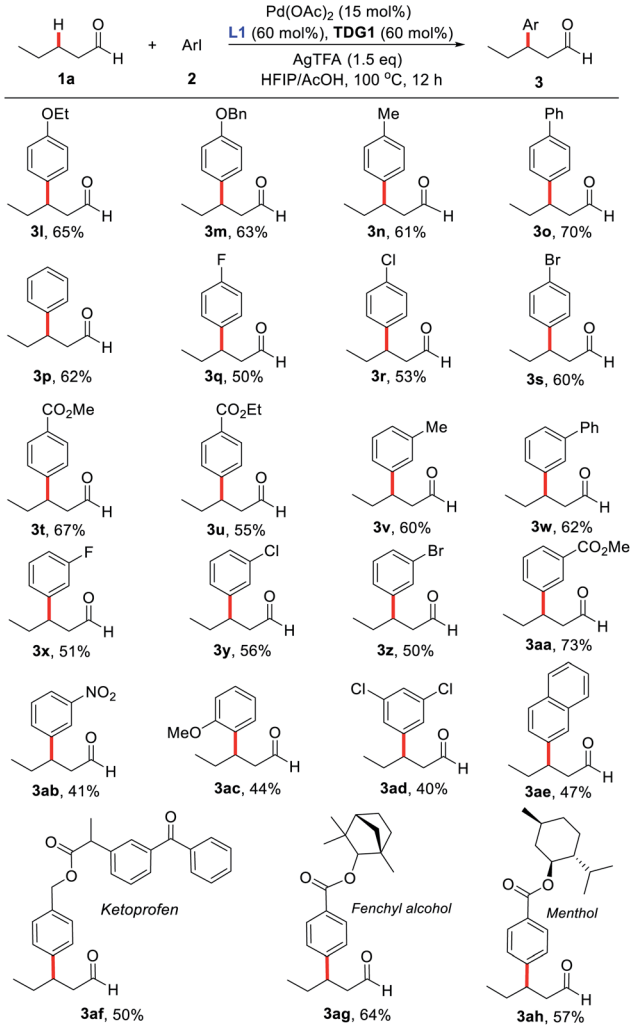

Scheme 4 Scope of aryl iodides. Reaction conditions: **1a** (0.2 mmol), **2** (0.4 mmol), $Pd(OAc)_2$ (15 mol%), AgTFA (0.3 mmol), **L1** (60 mol%), **TDG1** (60 mol%), HFIP (1.8 mL), HOAc (0.2 mL), 100 °C, 12 h. Isolated yields.

Density functional theory (DFT) calculations were performed to help investigate the reaction mechanism and to elucidate the role of the ligand in improving the reactivity (Fig. 2). The condensation of the aliphatic aldehyde **1a** with the **TDG** to form **imine-1a** was found thermodynamically neutral (ΔG° = −0.1 kcal mol^{-1}). As a result, it was permissible to use **imine-1a** directly in the calculations. According to the calculations results, the precatalyst $[Pd(OAc)_2]_3$, a trimeric complex, initially experiences dissociation and ligand metathesis with **imine-1a** to generate the Pd(II) intermediate **IM1**, which is thermodynamically favorable by 21.9 kcal mol^{-1}. Consequently, the deprotonated **imine-1a** couples to the bidentate ligand to form the stable six-membered chelate complex **IM1**. Therefore, **IM1** is indeed the catalyst resting state and serves as the zero point to the energy profile. We have identified two competitive pathways for the Pd(II)-catalyzed C–H activation starting from **IM1**, one of which incorporates **L1** and another which does not. On the one hand, an acetate ligand substitutes one **imine-1a** chelator in **IM1** to facilitate the subsequent C–H activation leading to **IM2**, which undergoes C(sp^3)–H activation through concerted metalation-deprotonation (CMD) *via* **TS1** ($\Delta G^\ddagger$ = 37.4 kcal mol^{-1}). However, this kinetic barrier is thought to be too high to account for the catalytic activity at 100 °C. On the other hand, the chelate **imine-1a** could be replaced by two N-coordinated ligands (**L1**) leading to the Pd(II) complex **IM3**. This process is endergonic by 6.4 kcal mol^{-1}. To allow the ensuing C–H activation, **IM3** dissociates one ligand (**L1**) producing the active species **IM4**, which undergoes **TS2** to cleave the β-C(sp^3)–H bond and form the [5,6]-bicyclic Pd(II) intermediate **IM5**. Although this step features an energy barrier of 31.2 kcal mol^{-1}, it is thought to be feasible under the experimental conditions (100 °C). Possessing similar coordination ability to that of pyridine, the ligand (**L1**) effectively stabilizes the Pd(II) center in the C–H activation process, indicating that this step most likely involves a manageable kinetic barrier. This result explicates the origin of the ligand-enabled reactivity (**TS2** *vs.* **TS1**). Additionally, we considered the γ-C(sp^3)–H activation pathway *via* **TS2′** which was found to have a barrier of 35.5 kcal mol^{-1}. The higher energy barrier of **TS2′** compared to that of **TS2** is attributed to its larger ring strain in the [6,6]-bicyclic Pd(II) transition state, which reveals the motive for the site-selectivity. Reverting back to the supposed pathway, upon the formation of the bicyclic intermediate **IM5**, it undergoes ligand/substrate replacement to afford intermediate **IM6**, at which the Ar–I coordinates to the Pd(II) center to enable oxidative addition *via* **TS3** ($\Delta G^\ddagger$ = 27.4 kcal mol^{-1}) leading to the five-coordinate Pd(IV) complex **IM7**. Undergoing direct C–C reductive elimination in **IM7** would entail a barrier of

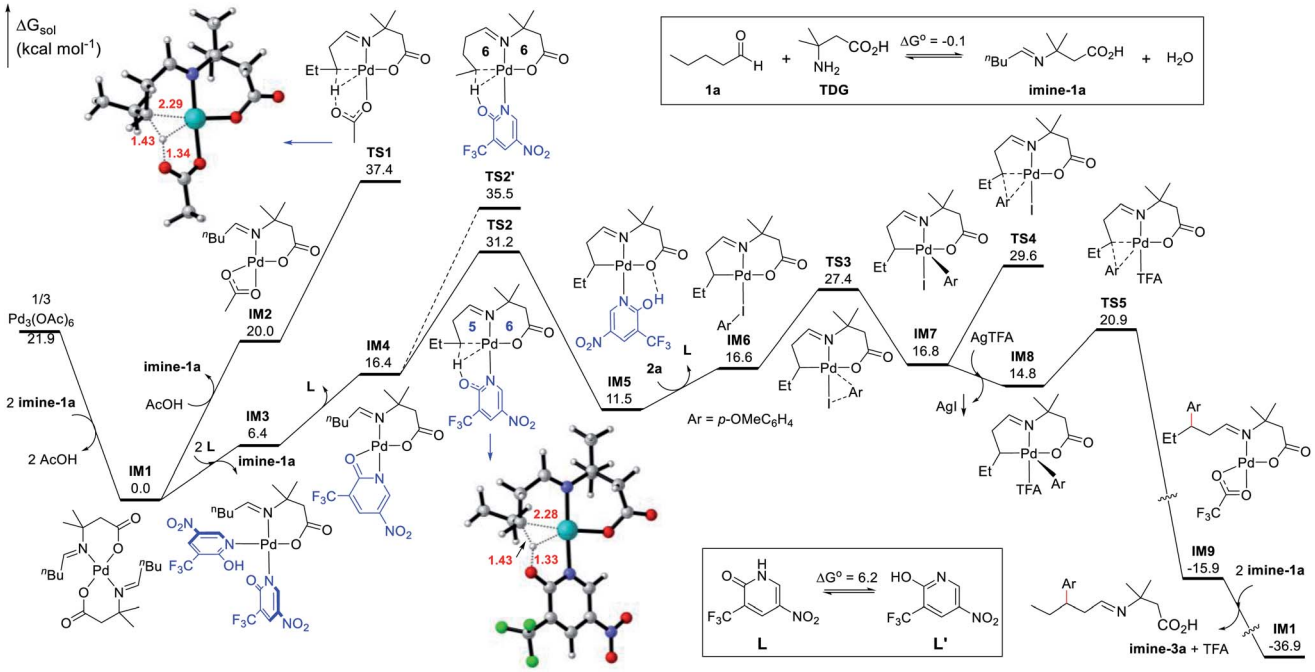

Fig. 2 Free energy profiles for the ligand-promoted Pd(II)-catalyzed site-selective C–H activation and C–C bond formation, alongside the optimized structures of the C–H activation transition states **TS1** and **TS2** (selected bond distances are labelled in Å). Energies are relative to the complex **IM1** and are mass-balanced.

29.6 kcal mol^{-1} (**TS4**). Alternatively, iodine abstraction by the silver(I) salt in **IM7** is thermodynamically favorable and irreversible, yielding the Pd(IV) intermediate **IM8** coordinated to a TFA ligand. Subsequently, C–C reductive coupling *via* **TS5** generates the Pd(II) complex **IM9** and concludes the arylation process. This step was found both kinetically facile (6.1 kcal mol^{-1}) and thermodynamically favorable (30.7 kcal mol^{-1}). Finally, **IM9** reacts with **imine-1a** *via* metathesis to regenerate the palladium catalyst **IM1** and release **imine-3a** in a highly exergonic step (21.0 kcal mol^{-1}). Ultimately, **imine-3a** undergoes hydrolysis to yield the aldehyde product **3a** and to release the TDG.

Conclusions

In summary, we have developed a palladium-catalyzed direct methylene β-C–H arylation of linear primary aliphatic aldehydes using commercially available 3-amino-3-methylbutanoic acid as a transient directing group and 3-(trifluoromethyl)-5-nitropyridin-2-ol as an external ligand. This reaction circumvents the requirement of having α–β-unsaturation, allowing direct β-C(sp^3)–H functionalization and granting much needed access to β-tertiary aldehydes with high site-selectivity and excellent functional group compatibility. In the case of arylation, the newly generated tertiary center is stereogenic, opening the door to future asymmetric synthetic applications *via* the use of chiral transient directing and external ligands, especially since DFT calculations suggest that both components are bound in the arylation step, promising adequate stereocontrol. Finally, the versatility of the aldehyde moiety and the endless transformation possibilities expand the synthetic utility of this method. Further studies are being conducted in our laboratory to develop new transformations and to explore the means of stereochemistry control over the newly generated chiral center.

Data availability

All experimental and computational data associated with this study are available in ESI.†

Author contributions

D. M. and H. G. conceived and designed the research. Y. D. performed theoretical calculations. K. Y. planned and performed the experiments. K. Y. also analyzed the experimental data. Z. L., C. L., Y. L., Q. H., B. L. and J. D. performed the experiments. K. Y., M. E. and H. G. wrote the manuscript.

Conflicts of interest

There are no conflicts to declare.

Acknowledgements

We gratefully acknowledge NSF (CHE-2029932), Robert A. Welch Foundation (D-2034-20200401), NSFC (No. 22073067), and Texas Tech University for financial support. Ke Yang is grateful for financial support from NSFC (No. 21702019) and Advanced Catalysis and Green Manufacturing Collaborative Innovation Center, Changzhou University. Ke Yang also

acknowledge the analytical testing support from Analysis and Testing Center, NERC Biomass of Changzhou University.

Notes and references

1 (*a*) A. Parenty, A. P. X. Moreau and J.-M. Campagne, *Chem. Rev.*, 2006, **106**, 911; (*b*) Y. Kim and P. Walsh, *Acc. Chem. Res.*, 2012, **45**, 1533.

2 (*a*) T.-Y. Luh, M.-K. Leung and K.-T. Wong, *Chem. Rev.*, 2000, **100**, 3187; (*b*) B. I. Roman, N. D. Kimpe and C. V. Stevens, *Chem. Rev.*, 2010, **110**, 5914.

3 (*a*) S. Mukherjee, J. W. Yang, S. Hoffmann and B. List, *Chem. Rev.*, 2007, **107**, 5471; (*b*) A. E. Allen and D. W. C. MacMillan, *Chem. Sci.*, 2012, **3**, 633.

4 For selected examples of using α,β-unsaturated aldehydes, see: (*a*) N. A. Paras and D. W. C. MacMillan, *J. Am. Chem. Soc.*, 2001, **123**, 4370; (*b*) J. F. Austin and D. W. C. MacMillan, *J. Am. Chem. Soc.*, 2002, **124**, 1172; (*c*) S. P. Brown, N. C. Goodwin and D. W. C. MacMillan, *J. Am. Chem. Soc.*, 2003, **125**, 1192; (*d*) Y. K. Chen, M. Yoshida and D. W. C. MacMillan, *J. Am. Chem. Soc.*, 2006, **128**, 9328; (*e*) I. Ibrahem, G. Ma, S. Afewerki and A. Córdova, *Angew. Chem., Int. Ed.*, 2013, **52**, 878.

5 For selected examples of using photocatalysis, see: (*a*) M. T. Pirnot, D. A. Rankic, D. B. C. Martin and D. W. C. MacMillan, *Science*, 2013, **339**, 1593; (*b*) J. A. Terrett, M. D. Clift and D. W. C. MacMillan, *J. Am. Chem. Soc.*, 2014, **136**, 6858.

6 (*a*) T. W. Lyons and M. S. Sanford, *Chem. Rev.*, 2010, **110**, 1147; (*b*) G. Rouquet and N. Chatani, *Angew. Chem., Int. Ed.*, 2013, **52**, 11726; (*c*) Z.-K. Chen, B.-J. Wang, J.-T. Zhang, W.-L. Yu, Z.-X. Liu and Y.-H. Zhang, *Org. Chem. Front.*, 2015, **2**, 1107; (*d*) J. He, M. Wasa, K. S. L. Chan, Q. Shao and J.-Q. Yu, *Chem. Rev.*, 2017, **117**, 8754.

7 (*a*) D. A. Colby, R. G. Bergman and J. A. Ellman, *J. Am. Chem. Soc.*, 2008, **130**, 3645; (*b*) S. Duttwyler, S. Chen, M. K. Takase, K. B. Wiberg, R. G. Bergman and J. A. Ellman, *Science*, 2013, **339**, 678.

8 (*a*) C.-L. Sun, N. Liu, B.-J. Li, D.-G. Yu, Y. Wang and Z.-J. Shi, *Org. Lett.*, 2010, **12**, 184; (*b*) Z. Yu, Y. Zhang, J. Tang, L. Zhang, Q. Liu, Q. Li, G. Gao and J. You, *ACS Catal.*, 2020, **10**, 203.

9 F. L. Zhang, K. Hong, T. J. Li, H. Park and J.-Q. Yu, *Science*, 2016, **351**, 252.

10 K. Yang, Q. Li, Y.-B. Liu, G. Li and H. Ge, *J. Am. Chem. Soc.*, 2016, **138**, 12775.

11 (*a*) Q. Zhao, T. Polsson, X. Pannecouke and T. Besset, *Synthesis*, 2017, **49**, 4808; (*b*) P. Gandeepan and L. Ackermann, *Chem*, 2018, **4**, 199; (*c*) T. Bhattacharya, S. Pimparkar and D. Maiti, *RSC Adv.*, 2018, **8**, 19456; (*d*) S. St John-Campbell and J. A. Bull, *Org. Biomol. Chem.*, 2018, **16**, 4582; (*e*) B. Li, K. Seth, B. Niu, L. Pan, H. Yang and H. Ge, *Angew. Chem., Int. Ed.*, 2018, **57**, 3401; (*f*) B. Niu, K. Yang, B. Lawrence and H. Ge, *ChemSusChem*, 2019, **12**, 2955; (*g*) K. Yang, M. Song, H. Liu and H. Ge, *Chem. Sci.*, 2020, **11**, 12616.

12 (*a*) S. St John Campbell, A. J. P. White and J. A. Bull, *Chem. Sci.*, 2017, **8**, 4840; (*b*) S. St John Campbell and J. A. Bull, *Chem. Commun.*, 2019, **55**, 9172; (*c*) B.-B. Gou, H.-F. Liu, J. Chen and L. Zhou, *Org. Lett.*, 2019, **21**, 7084; (*d*) X.-L. Zhang, G.-F. Pan, X.-Q. Zhu, R.-L. Guo, Y.-R. Gao and Y.-Q. Wang, *Org. Lett.*, 2019, **21**, 2731; (*e*) C. Dong, L. Wu, J. Yao and K. Wei, *Org. Lett.*, 2019, **21**, 2085.

13 (*a*) K. Hong, H. Park and J.-Q. Yu, *ACS Catal.*, 2017, **7**, 6938; (*b*) L. Pan, K. Yang, G. Li and H. Ge, *Chem. Commun.*, 2018, **54**, 2759; (*c*) J. Wang, C. Dong, L. Wu, M. Xu, J. Lin and K. Wei, *Adv. Synth. Catal.*, 2018, **360**, 3709.

14 (*a*) Y. Liu and H. Ge, *Nat. Chem.*, 2017, **9**, 26; (*b*) Y. Xu, M. C. Young, C. P. Wang, D. M. Magness and G. B. Dong, *Angew. Chem., Int. Ed.*, 2016, **55**, 9084; (*c*) Y.-W. Wu, Y.-Q. Chen, T. Liu, M. D. Eastgate and J.-Q. Yu, *J. Am. Chem. Soc.*, 2016, **138**, 14554; (*d*) A. Yada, W.-Q. Liao, Y. Sato and M. Murakami, *Angew. Chem., Int. Ed.*, 2017, **56**, 1073; (*e*) H. Lin, C. Wang, T. D. Bannister and T. M. Kamenecka, *Chem.–Eur. J.*, 2018, **24**, 9535; (*f*) M. Kapoor, D. Liu and M. C. Young, *J. Am. Chem. Soc.*, 2018, **140**, 6818; (*g*) S. St John-Campbell, A. K. Ou and J. A. Bull, *Chem.–Eur. J.*, 2018, **24**, 17838; (*h*) Z. Wang, Y. Fu, Q. Zhang, H. Liu and J. Wang, *J. Org. Chem.*, 2020, **85**, 7683.

15 (*a*) Y.-Q. Chen, Z. Wang, Y. Wu, S. R. Wisniewski, J. X. Qiao, W. R. Ewing, M. D. Eastgate and J.-Q. Yu, *J. Am. Chem. Soc.*, 2018, **140**, 17844; (*b*) Y.-Q. Chen, S. Singh, Y. Wu, Z. Wang, W. Hao, P. Verma, J. X. Qiao, R. B. Sunoj and J.-Q. Yu, *J. Am. Chem. Soc.*, 2020, **142**, 9966; (*c*) L.-J. Xiao, K. Hong, F. Luo, L. Hu, W. R. Ewing, K.-S. Yeung and J.-Q. Yu, *Angew. Chem., Int. Ed.*, 2020, **59**, 9594; (*d*) P. A. Provencher, J. F. Hoskin, J. J. Wong, X. Chen, J.-Q. Yu, K. N. Houk and E. J. Sorensen, *J. Am. Chem. Soc.*, 2021, **143**, 20035; (*e*) P. A. Provencher, K. L. Bay, J. F. Hoskin, K. N. Houk, J.-Q. Yu and E. J. Sorensen, *ACS Catal.*, 2021, **11**, 3115.

16 (*a*) F. Li, Y. Zhou, H. Yang, Z. Wang, Q. Yu and F.-L. Zhang, *Org. Lett.*, 2019, **21**, 3692; (*b*) S. St John-Campbell, A. J. P. White and J. A. Bull, *Org. Lett.*, 2020, **22**, 1807; (*c*) B. Li, B. Lawrence, G. Li and H. Ge, *Angew. Chem., Int. Ed.*, 2020, **59**, 3078.

17 (*a*) D.-H. Wang, K. M. Engle, B.-F. Shi and J. Q. Yu, *Science*, 2010, **327**, 315; (*b*) S. Bag, T. Patra, A. Modak, A. Deb, S. Maity, U. Dutta, A. Dey, R. Kancherla, A. Maji, A. Hazra, M. Bera and D. Maiti, *J. Am. Chem. Soc.*, 2015, **137**, 11888; (*c*) T. Patra, S. Bag, R. Kancherla, A. Mondal, A. Dey, S. Pimparkar, S. Agasti, A. Modak and D. Maiti, *Angew. Chem., Int. Ed.*, 2016, **55**, 7751; (*d*) P. Wang, M. E. Farmer, X. Huo, P. Jain, P.-X. Shen, M. Ishoey, J. E. Bradner, S. R. Wisniewski, M. E. Eastgate and J. Q. Yu, *J. Am. Chem. Soc.*, 2016, **138**, 9269; (*e*) P. Wang, P. Verma, G. Xia, J. Shi, J. X. Qiao, S. Tao, P. T. W. Cheng, M. A. Poss, M. E. Farmer, K. S. Yeung and J. Q. Yu, *Nature*, 2017, **551**, 489; (*f*) R.-Y. Zhu, Z.-Q. Li, H. S. Park, C. H. Senanayake and J.-Q. Yu, *J. Am. Chem. Soc.*, 2018, **140**, 3564; (*g*) G. Xia, Z. Zhuang, L.-Y. Liu, S. L. Schreiber, B. Melillo and J.-Q. Yu, *Angew. Chem., Int. Ed.*, 2020, **59**, 7783; (*h*) H. S. Park, Z. Fan, R.-Y. Zhu and J.-Q. Yu, *Angew. Chem., Int. Ed.*, 2020, **59**, 12853.

18 Y.-H. Li, Y. Ouyang, N. Chekshin and J.-Q. Yu, *J. Am. Chem. Soc.*, 2022, **144**, 4727.